ACADEMIC PRESS

Available online at www.sciencedirect.com

SCIENCE DIRECT®

VIROLOGY

Virology 316 (2003) 234–244

www.elsevier.com/locate/yviro

Completion of trimeric hairpin formation of influenza virus hemagglutinin promotes fusion pore opening and enlargement

E. Borrego-Diaz,[a,1] M.E. Peeples,[b] R.M. Markosyan,[a] G.B. Melikyan,[a] and F.S. Cohen[a,*]

[a] *Department of Molecular Biophysics and Physiology, Rush Medical College, 1653 W. Congress Parkway, Chicago, IL 60612, USA*
[b] *Department of Immunology/Microbiology, Rush Medical College, 1653 W. Congress Parkway, Chicago, IL 60612, USA*

Received 27 May 2003; returned to author for revision 21 July 2003; accepted 25 July 2003

Abstract

For influenza virus hemagglutinin, an N-cap structure, created at low pH, interacts with membrane-proximal residues (173–178), bringing fusion peptides and membrane-spanning domains close together. Mutational analysis was used to define the role of these interactions in membrane fusion. For all N-cap mutants, both lipid and aqueous dye spread was greatly reduced. Mutation at residues that interact with the N-cap did not reduce levels of fusion, except for substitutions made at residue I173. For N-cap and I173 mutants, the addition of chlorpromazine greatly promoted transfer of aqueous dye. Electrical capacitance measurements confirmed that fusion pores usually did not form for the I173 mutants. Thus, neither N-cap formation nor interactions with segment 173–178 are needed for hemifusion, but are required for reliable formation and enlargement of the fusion pore. It is proposed that binding of I173 into a deep hydrophobic cavity within the coiled-coil promotes the transition from hemifusion to fusion.

Keywords: Membrane fusion; Six-helix bundles; Capacitance measurements; Fluorescence microscopy; Hemifusion; Fusion peptides

Introduction

Fusion of a viral envelope with a cell membrane is the event that allows the transfer of a viral genome into the cytosol of an infected cell. For influenza virus, the protein in the envelope responsible for membrane fusion is hemagglutinin (HA). HA is a homotrimer, each monomer consisting of two subunits, HA1 and HA2. HA1 binds influenza to cells, and HA2 is the subunit that induces membrane fusion. For viral fusion proteins in general, the fusion proteins are trimers and the majority of the protein lies outside the virus and is known as the ectodomain. Each monomer of the subunit responsible for fusion contains a “fusion peptide” and a single transmembrane domain (TMD). Fusion peptides are stretches of about 20 nonpolar amino acid residues that insert into the target membrane during fusion (Durrer et al., 1996; Hernandez et al., 1996; Stegmann et al., 1991).

More is known about HA’s conformational changes during fusion than is known for any other fusion protein. Influenza virus is internalized into cells by endocytosis, and the low pH of the endosome triggers conformational changes in HA that culminate in fusion. The structure of the ectodomain of HA has been crystallographically determined in its uncleaved form (Chen et al., 1998), its native cleaved neutral-pH form (Wilson et al., 1981 Skehel, and Wiley, 1981), as well as its low-pH, postfusion form (Bullough et al., 1994; Chen et al., 1999). The final, postfusion form of ectodomains (or peptide fragments of them) for many proteins from diverse viral families have also been determined. Thus we know that the ectodomains of fusion proteins from many viruses—including HA of influenza, HIV-1 (Chan et al., 1997; Weissenhorn et al., 1997), simian immunodeficiency virus (Caffrey et al., 1998), human T-cell leukemia virus (Kobe et al., 1999), Moloney murine leukemia virus (Fass et al., 1996), Ebola virus (Eckert et al., 1999; Weissenhorn et al., 1998), and the paramyxoviruses SV5 (Baker

* Corresponding author. Fax: +1-312-942-8711.
E-mail address: fcohen@rush.edu (F.S. Cohen).
[1] Present address: Boston Biomedical Research Institute, 64 Grove Street, Watertown, MA 02472.

0042-6822/$ – see front matter © 2003 Elsevier Inc. All rights reserved.
doi:10.1016/j.virol.2003.07.006

et al., 1999) and respiratory syncytia virus (Zhao et al., 2000)—exhibit great structural similarity. Typically, there is a central core of a triple-stranded coiled-coil formed from N-terminal α-helices. This creates three grooves into which the three C-terminal α-helices pack antiparallel to the central core. For many of the proteins, the C-terminal segments fit as α-helices into the grooves of the central triple-stranded coiled-coil, yielding the rod-like structure of a six-helix bundle. For proteins that have only short stretches between both the TMD and C-terminal helices, and between the fusion peptide and the coiled-coil, formation of the six-helix bundle alone brings the fusion peptides and TMDs into close proximity as a direct consequence of the antiparallel arrangement of the N- and C-terminal α-helices (Baker et al., Skehel and Wiley, 2000; Eckert and Kim, 2001). But HA2 has a lengthy stretch of amino acids between the short C-terminal helices of the six-helix bundle and the TMDs. The crystal structure shows, however, that the fusion peptides and TMDs should still come into close proximity. The lengthy stretch of amino acids runs as an extended chain along the grooves of the coiled-coil, and residues toward the C-termini of this extended conformation bond with N-terminal residues that end the α-helices of the central coiled-coil core (Chen et al., 1999). The structure formed by the residues at the N-terminus of the α-helices is known as an "N-cap."

Clearly, the absence of successive residues (as part of the helix) at the ends of an α-helix prevents the main-chain carbonyl oxygens and amide hydrogens from forming as many hydrogen bonds with each other as those internal to the helix. As a result, for many α-helices the side chains of the end residues loop back to bond to adjacent residues of the helix and when they do, the α-helix is terminated in a way that prevents its unraveling (Presta and Rose, 1988; Richardson and Richardson, 1988). In the case of HA at low pH, residues at the N-terminus of the coiled-coil (explicitly, residues 34–37) interact not only with adjacent residues of their own α-helices, but also with residues of the other two helices. Residues 34–37 thereby form an N-cap structure that both terminates the individual α-helices and serves to tie the three helices of the coiled-coil together. The fusion peptide of HA is at the N-terminus (residues 1 through 20) and is therefore close to the N-cap structure. The residues of the C-terminal chain that interact (residues 173–178, which we refer to as the N-cap interacting residues or "NCI residues") with residues of the N-cap are similarly close to the TMD (residues 186–212). Consequently, the fusion peptides and the TMDs must be in close proximity and might even intermingle in the final HA structure. When the extended chains are within the grooves and the NCI residues interact with the N-cap, we refer to the structure as a "trimeric hairpin."

Proximity of the fusion peptides and TMDs is generally thought to be critical to viral fusion (Cohen, 2002; Ferrer et al., 1999). For intracellular fusion, proximity of TMDs of SNAREs, comprising tetrameric coiled-coils, inserted in opposite membranes is also thought to be essential for fusion (McNew et al., 2000; Sutton et al., 1998). However, it is not known where, in the multistep process of viral membrane fusion, proximity of fusion peptides and TMDs is achieved and if it is truly an important factor. Since proximity between fusion peptides and TMDs of HA is effected by interactions between very discrete regions—the N-cap and residues 173–178 (Chen et al., 1999)—the energies of these interactions can be substantially reduced by site-directed mutagenesis. Through this approach, we show that neither the N-cap nor the NCI residues are needed to achieve hemifusion (the merger of contacting, proximal monolayer leaflets of membranes). But the N-cap and a particular NCI residue, I173, promote fusion pore formation and enlargement. We propose that it is the interaction between the N-cap and I173 that promotes the steps downstream of hemifusion.

Results

Selecting sites for specific mutations

For HA2 at low pH, residues that are part of and adjacent to the N-cap interact extensively with residues 173–178 (Chen et al., 1999). We aligned sequences of HA from 14 subtypes of influenza virus and found that Ala35, Ala36, and Asp37 are conserved, as noted previously (Chen et al., 1999), but that residue 34 (Gln for X:31 HA used in this study) is not. Also conserved are Ser40 and Thr41, which are part of the α-helices terminated by the N-cap. Alignment also shows that Ile173, Val176, and Leu178 (residues that interact with the N-cap) are conserved with exception of isolated variations. The precise structures of the N-cap and the NCI region, or their interactions, are presumed to be essential in fusion (Chen et al., 1999); this is supported by the high degree of conservation in a highly mutating protein. We introduced either single or double mutations at residues 35–37, choosing amino acids known to statistically disfavor formation of N-caps (Richardson and Richardson, 1988). We also mutated the NCI residues that are hydrophobic and conserved (residues 173, 176, and 178) to residues with polar side chains so as to hinder interactions with the N-cap. We initially made the mutations I173E, V176E, and L178Q and found that only I173E had a dramatic effect on fusion. We therefore made several other mutations at position 173. We also deleted the region 173–178.

Cell surface expression, cleavage, and conformational changes in mutant HA

Wild-type HA (wt HA) and each mutant were expressed in cells by transfection. In order to compare the ability of a mutant HA to induce fusion with the ability of wt HA, it was necessary to express them with comparable densities. This was done by manipulating the amount of DNA used and,

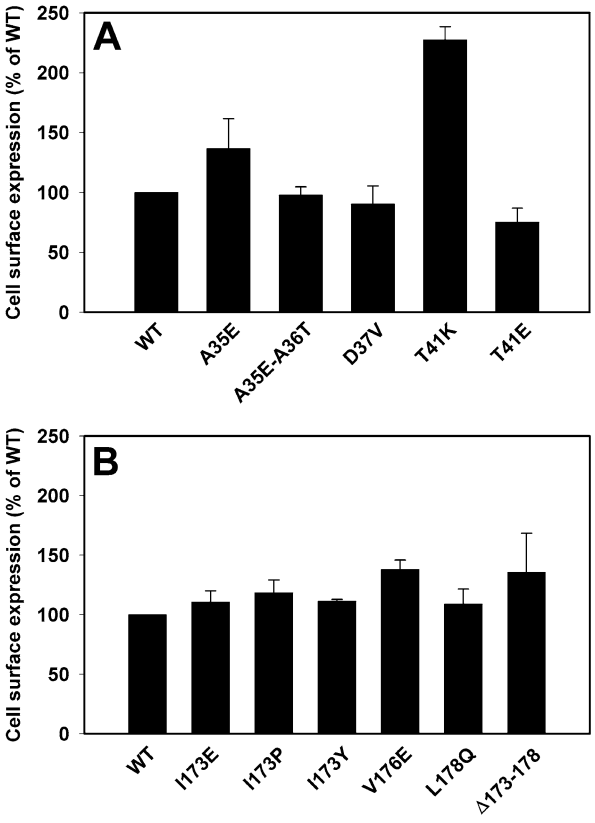

Fig. 1. Cell surface expression of wt HA and mutants. (A) N-cap mutants. (B) N-cap interacting residue (NCI residue) mutants. In all cases, mutants were expressed on cell surfaces at comparable or greater levels, as determined by FACS analysis. Error bars are SEM from at least three independent experiments.

when necessary, elevating expression levels of a mutant by adding sodium butyrate to the cell culture medium 18 h prior to use (Danieli et al., 1996). Cell surface expression levels (Fig. 1) were measured by flow cytometry (FACS) (see Materials and methods) or alternatively were assessed by a cell-ELISA assay (data not shown). FACS and ELISA measurements yielded the same comparative expression levels between mutants. For all the mutants, both those within the N-cap itself (Fig. 1A) and the NCI residues (Fig. 1B), conditions were adjusted to yield expression levels similar to that of wt HA. Because mutations at I173 were deleterious to fusion, we also expressed I173E at three times the level of wt HA and observed improved fusion, but the extent of fusion was still much less than that for wt HA (see Fig. 6).

HA was expressed on the 293T cell surfaces in its uncleaved HA0 form. Treating the cells with small amounts of trypsin properly cleaved wt HA0 at a single site (Fig. 2). If a mutated HA misfolds, sites susceptible to cleavage by trypsin tend to become exposed, and this provides a means to test for proper folding. In order to determine whether HA on the surface of the cells had been properly cleaved by trypsin, it was necessary to exclude from analysis any HA located in intracellular pools, such as Golgi. We accomplished this by biotinylating surface proteins (Qiao et al., 1999). Cells were then treated with trypsin, HA was immunoprecipitated by an anti-HA1 antibody, and the immune complexes were subject to Western blot analysis. By binding strepavidin–HRP, the biotinylated HA0 as well as the cleaved HA1 subunit were identified. Because the anti-HA1 antibody did not bind to HA2, HA2 is never present in the gel. Wild-type and all point mutants (except for T41K and T41E) were properly cleaved by trypsin (Fig. 2), indicating that they had folded properly. T41K and T41E were more severely digested by trypsin, demonstrating some misfolding. We therefore do not further pursue the consequences of mutation at residue 41 on fusion.

The deletion mutant Δ173–178 appeared to be properly folded, although some surface HA0 was cleaved without adding trypsin, showing that this mutant was more readily cleaved by intracellular proteases than was wt HA. Thus, either slight misfolding occurred or the absence of residues 173–178 facilitated exposure of the cleavage site during intracellular transport. The fraction of the deletion mutant that did reach the cell surface in its HA0 form was properly cleaved by external trypsin.

We determined whether the mutants underwent proper conformational changes at low pH, using an antibody (CHA-1) that recognizes an epitope that is normally only exposed at low pH (White and Wilson, 1987). We measured antibody binding by cell-ELISA and found that all the point mutants underwent pH-dependent conformational changes similar to that of wt HA (Fig. 3). For mutations within the N-cap, the pH dependences of these changes were somewhat less steep than that of wt HA (Fig. 3A). Mutations at I173 did not alter at all the pH dependence for conformational changes (Fig. 3B). Having established that mutants were expressed well, that most were properly folded, and that they underwent appropriate low-pH conformational changes, we determined their ability to induce fusion. In the cases in which fusion was impaired, we determined how far in the process fusion had proceeded.

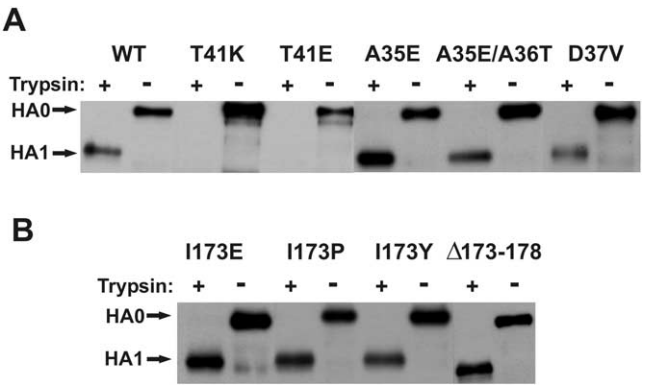

Fig. 2. SDS–PAGE of HA cleaved by trypsin. (A) N-cap mutants. (B) Mutations at I173 and deletion of the NCI residues; see Materials and methods for details. Separate gels were cut and pasted for visual display.

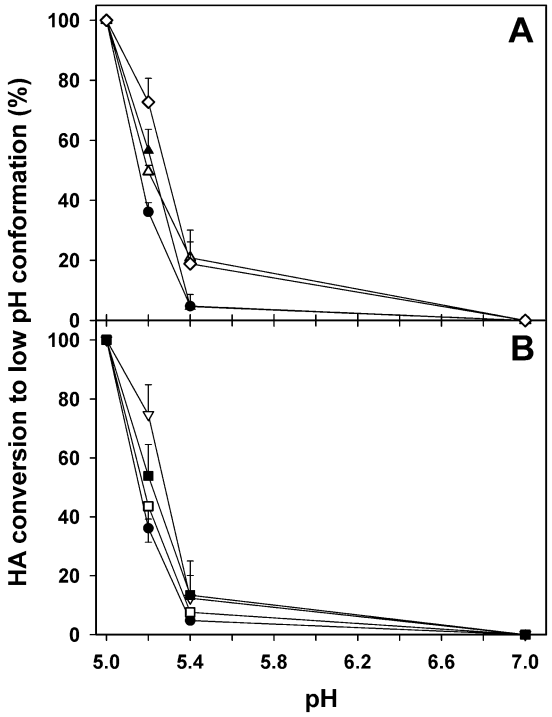

Fig. 3. The pH dependence of conformational changes in HA and mutants is shown for (A) N-cap mutants (wt HA, filled circles; A35E, open triangles; A35E-A36T, filled triangles; D37V, open diamonds) and (B) mutations at residue I173 (wt HA, filled circles; I173E, open inverted triangles; I173P, open squares; I173Y, filled squares). Each curve was generated from at least three experiments.

Fusion activity

Fusion between HA-expressing cells and RBCs was triggered by lowering pH. Fig. 4 compares the behavior of wt HA and two mutants, one within the N-cap, D37V, and one NCI residue mutant, I173P. For wt HA, both R18 and CF transferred after lowering of pH, showing that full fusion resulted. However, neither appreciable lipid mixing nor content mixing occurred for either mutant. It is thought that hemifusion is an intermediate stage of fusion (Cohen, 2002), and at this stage lipid movement is restricted (Chernomordik et al., 1998). The restriction of lipid dye movement may be due to the high density of HA at the site of hemifusion, which would occlude the passage of lipid (Chernomordik et al., 1998). The existence of this hemifusion stage is inferred if the addition of chlorpromazine (CPZ)—a membrane-permeable weak base that preferentially partitions into inner leaflets of cell membranes—leads to full fusion (Chernomordik et al., 1998; Melikyan et al., 1999, 2000a). (When hemifusion diaphragms are known to exist, CPZ disrupts them (Melikyan et al., 1997).) For both mutants, the addition of CPZ induced lipid and aqueous dye spread. Content mixing after the addition of CPZ indicates that, for these mutants, fusion had become arrested at a state of hemifusion in which lipid movement was restricted. As a consequence of mutation, the process did not continue on to full fusion.

These procedures of testing for hemifusion and/or fusion were extended to include all the mutants that expressed, folded correctly, and underwent appropriate low pH-dependent conformational changes. The percentage of the HA-expressing cells with bound RBCs that became stained by R18 (Figs. 5 and 6, filled bars) and by CF (open bars) after lowering of the pH is shown for these mutants. All the mutations within the N-cap region were deleterious to both lipid and aqueous dye spread (Fig. 5A); within the region 173–178, only mutations at position 173 were particularly destructive (Fig. 6A). All of the N-cap mutants, except A35E, exhibited less than 30% of the lipid-mixing activity of wt HA and the level of content mixing was even more reduced. After adding CPZ, content mixing comparable to that of wt HA was observed for all the mutants (Fig. 5B). It is particularly notable that all mutant HA-expressing cells with a bound RBC that did not exhibit dye transfer after lowering of pH did display contents mixing after the addition of CPZ. We conclude that the mutant HA cell and RBC membranes were in a state of local hemifusion prior to the addition of CPZ. For wt HA, this state of hemifusion transits to full fusion.

Mutating the NCI residue 173 had a greater effect on content mixing than did mutating residues of the N-cap itself. The single mutants I173Y, I173P, and I173E exhibited negligible content mixing (Fig. 6B). The point mutations V176E and L178Q did not significantly affect fusion. Thus, whereas mutation anywhere within the N-cap region tended to inhibit fusion, mutation within the interacting C-terminal region that reduced fusion was localized to residue 173. The addition of CPZ augmented content mixing for all the NCI residue mutants tested, usually to the maximum extent possible (Fig. 6B).

To determine whether mutants at I173 could support any fusion, we focused on I173E, because this mutant yielded the greatest evidence of some fusion activity. We expressed I173E to three times the surface density of wt HA. Lipid dye spread for the overexpressed mutant was comparable to that of wt HA (Fig. 6A, third open bar). The extent of aqueous dye spread was now significant, but was still only about 30% of wt HA. It is striking that point mutations at a single residue, I173, could completely abolish aqueous dye spread. But clearly, fusion could be restored, at least to some extent, by expressing an I173 mutant at higher density. We did not explore whether fusion continued to increase with expression levels to the point that eventually all cells would be able to fuse.

Even when an aqueous dye does not transfer, it remains possible that a pore too small to allow dye spread has formed. We used the patch clamp technique to perform electrical capacitance measurements to check for this possibility, as capacitance measurements present the most sensitive assay available to detect fusion pores. In 4 of 17 experiments using I173E expressed at the same density as

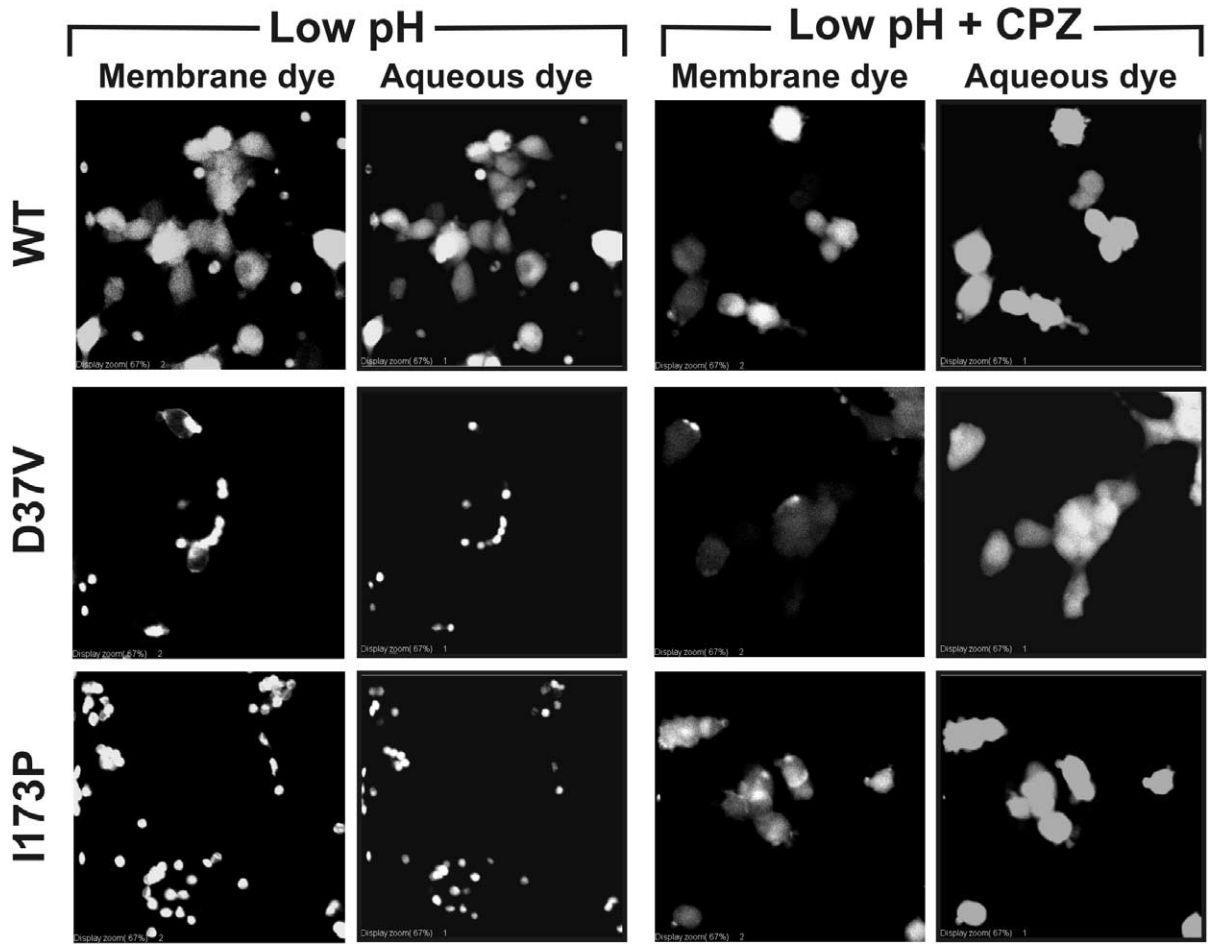

Fig. 4. Images for the spread of membrane (R18) and aqueous (CF) dye from RBCs to HA-expressing cells for wt HA, D37V, and I173P. After low pH, both dyes spread well for wt HA, but remained confined for both mutants (left columns). After addition of 0.5 mM CPZ for 1 min to solution, dyes spread for both mutants (right columns). The dull appearance of R18 is due to its quenching by CPZ (31).

that in wt HA, we observed a small pore that did not enlarge and was too small to allow for the passage of dye (Fig. 7, bottom trace). In the remaining 13 experiments, no pores formed (middle trace). In contrast, for wt HA, a pore almost always formed and enlarged (top trace). Taken together, our results strongly indicate that the N-cap is critical to fusion and that this structure must properly interact with I173 for the transition from hemifusion to full fusion.

Discussion

The trimeric hairpin of HA is analogous to the six-helix bundle of other fusion proteins

Our data show that the N-cap, and its ability to interact with residue I173, is critical for ensuring the transition from hemifusion to fusion. The data also indicate, based on CPZ sensitivity, that the stages up to and including hemifusion occur without the participation of the N-cap or its interactions with NCI residues. The blocking of fusion caused by mutation at I173 could be partially overcome by overexpressing the mutant. It is often the case that for an inhibitory effect on fusion to be observed, suboptimal fusion conditions must be employed: conditions that promote fusion can generally be made so optimal that the inhibitory effect can be overcome. For instance, incorporation of lysophosphatidylcholine into outer monolayer leaflets of membranes inhibits hemifusion and thereby blocks fusion. But suboptimal conditions are generally needed in order to clearly discern the inhibition (Chernomordik et al., 1998). It is thus not surprising that very high expression levels of a mutant can obscure the fact that the site of mutation is in fact critical.

Fusion peptides insert into target membranes at low pH (Durrer et al., 1996) and TMDs span the HA-expressing membrane. Based on crystal structures of fusion proteins in their postfusion form, these two membrane-spanning domains should come close to each other and, in so doing, would bring the two membranes into apposition (Eckert and Kim, 2001; Skehel and Wiley, 2000). We have hypothesized that bringing together the TMDs and fusion peptides not only places the membranes in close apposition, but it is

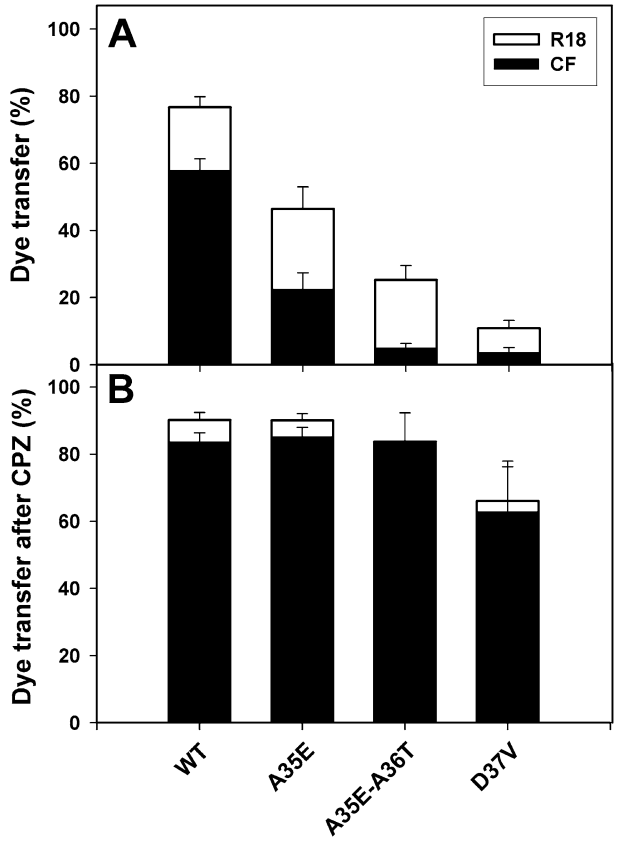

Fig. 5. Extents of fusion for N-cap mutants. (A) R18 (open bars) and CF (filled bars) transfers were less for all mutants than for wt HA. (B) After addition of CPZ, dye transfer was comparable for mutants and wt HA. Error bars are SEM for at least four experiments.

also the event that disrupts the hemifusion diaphragm to cause pore formation. (Markosyan et al., 2000; Melikyan et al., 1999, 1995). For several fusion proteins, such as HIV-1 Env, formation of the six-helix bundle forces the TMDs and fusion peptides into proximity. This is not the case for HA, because there is a long, extended chain between the outer helices of the six-helix bundle and the TMDs; the trimeric hairpin of HA is the structure whose formation brings the two membrane-inserted domains into proximity. Therefore, in terms of function, the trimeric hairpin of HA is analogous to the six-helix bundle of HIV-1 Env. For HIV-1 and SV5 fusion proteins, the six-helix bundle does not form until after membrane merging has occurred (Melikyan et al., 2000b; Markosyan, 2003; Russell et al., 2001). From the present study we can similarly conclude that the trimeric hairpin of HA does not form until after the membrane merger. But because the six-helix bundle of HA is physically far from the TMDs, it remains possible that the bundle forms prior to hemifusion (as illustrated in Fig. 8).

The structural alterations caused by mutation were local

Our mutations inhibited fusion through local alterations of HA, not through any global deleterious effects: the mutants were expressed well on cell surfaces, were properly cleaved into HA1–HA2 subunits, and underwent low pH-induced conformational changes. Every point mutation we made in the N-cap (that was cell surface expressed) reduced fusion; for cells that did not fuse, the fusion process was always arrested at the same point: at a CPZ-sensitive state. If mutations within the N-cap caused different, scattered conformational changes throughout HA, one would expect that fusion would become arrested at different points, depending on the precise mutation. But the process was consistently stopped at a CPZ-sensitive state, regardless of the precise mutation, which supports our conclusion that the N-cap participates in the fusion process only after hemifusion has been achieved.

The sequence of intermediate states of membrane fusion agrees with the expected sequence of HA structural changes

At neutral pH, the triple-stranded coiled-coil of HA2 is not terminated by an N-cap. The three “A”-helices, one from each monomer of HA, have not yet folded into a

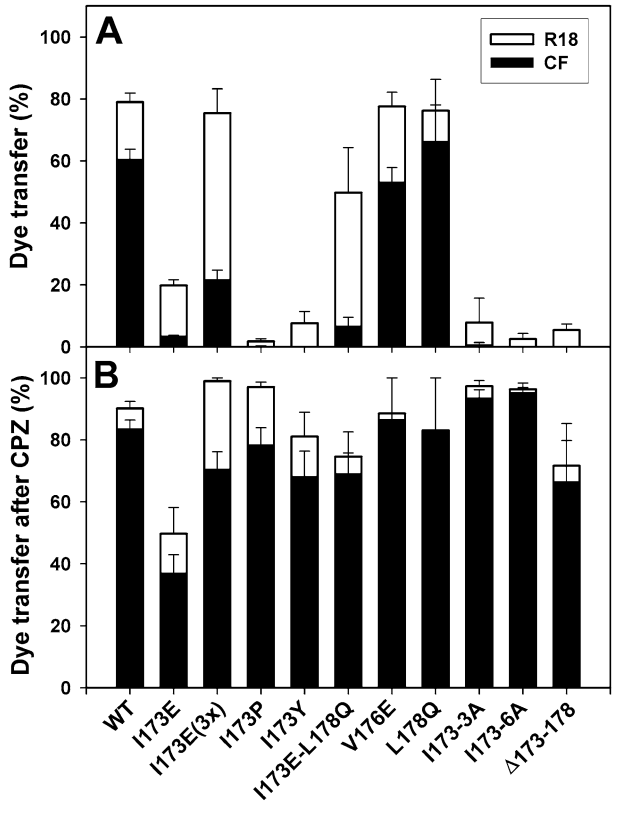

Fig. 6. Extents of fusion for NCI residue mutants. (A) R18 (open bars) and CF (filled bars) transfers were most affected when residue I173 was mutated. Expressing I173E at three times the surface concentration of wt HA (I173E(3x)) partially restored fusion activity. (B) After addition of CPZ, dye transfer was substantial for all mutants, even when all NCI residues were mutated to alanine (I173–6A) or deleted altogether (Δ173–178). Error bars are SEM for at least three experiments.

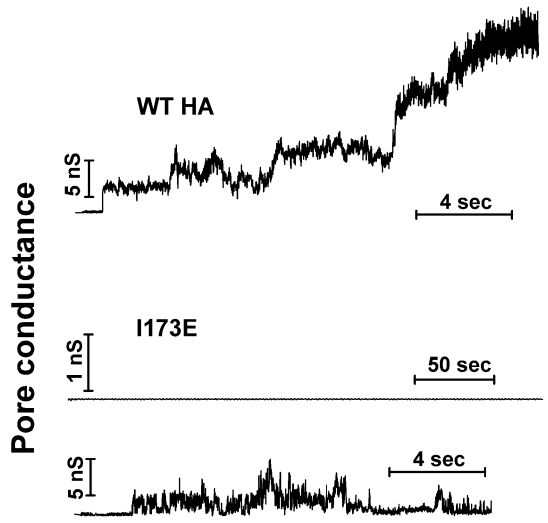

Fig. 7. Electrical measurements of fusion pores. (Top trace). Pores were observed in 7 of 8 experiments for wt HA and these pores always enlarged (Top trace). Pores were generally not induced by 1173E (middle trace), and when they were (in 4 of 17 experiments), they tended to close and never enlarge (bottom trace).

coiled-coil (Fig. 8). For the A-helices to become part of the coiled-coil, they must come together. This requires that each B-loop reconfigure from its disordered arrangement at neutral pH to an α-helix at low pH that becomes part of the extended coiled-coil. It is only after the A-helices have become part of the coiled-coil that the N-cap can form to tie them together. Therefore, one would expect that when N-cap formation is blocked or when its interactions with NCI residues are reduced, fusion proceeds further than when B-loop conversion is hindered. Mutations have been made that prevent B-loop conversion, and they abolish both fusion and the creation of CPZ-sensitive states (Gruenke et al., 2002; Qiao et al., 1998). That is, the formation of the extended coiled-coil is necessary for hemifusion to occur. We have found that mutations of the N-cap allow CPZ-sensitive states to form and that mutation of NCI residues allowed fusion to occur—except for mutation of I173, which allowed fusion to proceed only up to a CPZ-sensitive state. This is in accord with the order that conformational changes of HA are expected to occur.

Residue I173 is critical for the formation and growth of fusion pores

Mutation in the 173–178 region did not reduce fusion, with the exception of one location. It is striking that mutation at this residue, I173, could be so critical to the fusion process. All mutations we made at residue I173 reduced fusion, and in all cases fusion advanced up to a CPZ-sensitive state, but generally no further. Even when a small fusion pore was detected by electrical measurements, it closed or did not enlarge.

Why might I173 be so critical? Based on structure, we suggest that it is critical not only because it interacts with the N-cap (as other NCI residues also do), but also because it binds into a hydrophobic pocket, immediately adjacent to the N-cap, of the extended coiled-coil. Previous research has demonstrated that, for HIV-1 Env, the insertion of C-terminal residues into the cavity of a coiled-coil to make hydrophobic contacts is essential for fusion (Chan et al., 1998). For HA at low pH, there are nonpolar contacts between I173 and the N-cap. But the side chain of each I173 also fits into a hydrophobic pocket, created by T41, Q42, and F45, within each groove of the coiled-coil; hydrogen bonds between I173 and Q42 may help guide each I173 side chain into its respective pocket (Fig. 9). I173 is unique among the NCI residues in its ability to fit into a hydrophobic cavity. Of the conserved NCI residues, V176 and L178 also interact with the N-cap, but they are positioned beyond the coiled-coil and cannot pack into a groove. The N-cap appears to form a hydrophobic wall at the end of the pocket, extending the hydrophobic surface beyond the pocket. In this way, the N-cap shields the pocket from water, and this may facilitate the hydrophobic binding of I173. It is possible that the process occurs in the reverse order: I173 once bound into the pocket of the coiled-coil might serve as a nucleating center for N-cap formation. Alternatively, N-cap formation and I173 binding may be a cooperative process, occurring either sequentially or simultaneously. It may even be that the pocket cannot form independently with its hydrophobic surface exposed to water and that, in fact, it forms around I173. The absence of I173 would thereby destabilize the coiled-coil in the vicinity of the unformed pocket.

The structural importance of the N-cap can be appreciated when one compares the crystal structure of the fragment (EHA_2, residues 23–185) that revealed the N-cap (Chen et al., 1999) to the crystal structure as originally determined, the low-pH fragment ($TBHA_2$, residues 38–175) that does not contain the N-cap (Bullough et al., 1994). In the absence of the N-cap, the extended C-terminal segments are not packed into the grooves, and the stretch of residues 162–175 is not structured; without the N-cap, it is not apparent that the fusion peptides and TMDs would come close to each other. The more complete, more recent crystal structure (Chen et al., 1999) demonstrates that packing of the C-terminal segments into the grooves of the coiled-coil requires the existence of the N-cap and binding of I173. Based on the crystal structure, this packing seems to be highly dependent upon hydrophobic binding at a few discrete sites, rather than upon binding along the entire chain; I173 binds to one of these sites and the next critical location appears to fall at the Y162 binding site.

There are two HA2 trimers in the crystal, and segment 173–178 is disordered in five of the six monomers. The segment 173–178 of the sixth monomer has more hydrogen bonds, conferring greater order and appears to form a β-sheet. The actual conformation of the 173–178 segment may therefore fluctuate. The ability of the N-cap and I173

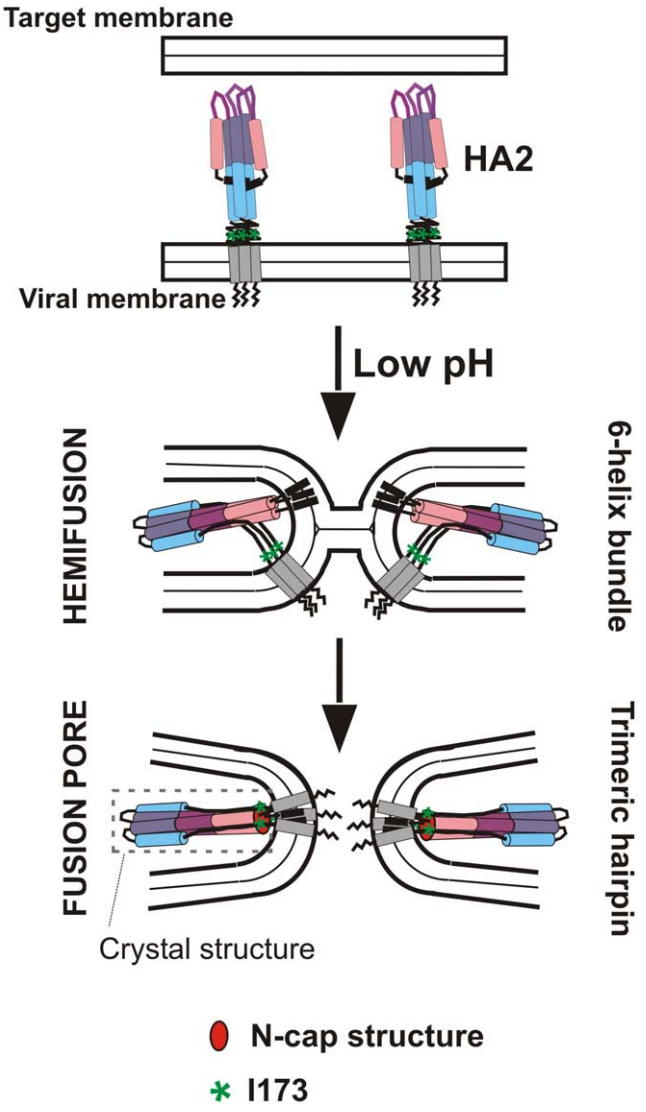

Fig. 8. Model of HA-induced fusion. The HA2 subunit is shown in schematized form; HA1 is omitted for visual clarity. As is known from crystallography (Bullough et al., 1994; Chen et al., 1999), the C helix (dark blue) and the D helix (light blue) of each monomer form a continuous α-helix in the native state (top). These helices form the central triple-stranded coiled-coil. Helix A (pink) is antiparallel to this coiled-coil and is connected by the B-loop (purple). After lowering of the pH (middle), the B-loop becomes an α-helix. As a result A, B, and C helices become one continuous α-helix that forms an extended coiled-coil. This allows the fusion peptide (bold black) to insert into the target membrane. Residues in the middle of the continuous C and D helices become random-coil and the D-helices pack antiparallel against the C-helices to form a six-helix bundle. Although this is not adequate to bring fusion peptides and TMDs (gray) toward each other, hemifusion nevertheless occurs. Only after the N-cap (red ellipse with black border) and I173 (green asterisk in all three panels) interact with each other do the TMDs and fusion peptides come into close proximity, allowing pore formation and enlargement. The N-cap cannot form until after the B-loop has become α-helical; the six-helix bundle must form for 1173 to interact with the N-cap. The crystallographic low-pH structure with N-cap is indicated by dashed box.

interactions to promote pore formation may be aided by free energy released by a favorable conformational transition of the 173–178 segment.

The TMD and fusion peptides must interact for fusion pore formation to occur

GPI-anchored ectodomains of HA have been molecularly engineered (Kemble et al., 1993) that contain residue I173. GPI-HA exhibits lipid dye spread at low pH (Kemble et al., 1994; Melikyan et al., 1995), with pore formation much more difficult to produce than for wt HA, and any pores that do form do not enlarge (Frolov, 2000; Markosyan et al., 2000). This is consistent with our central hypothesis that reliable pore formation and enlargement requires that the TMDs and fusion peptides approach each other subsequent to hemifusion.

A mutation within the TMD of an H2 subtype of HA has also been shown to induce a CPZ-sensitive state, but not pore formation (Melikyan et al., 2000a). This observation supports the notion that cooperative actions between TMDs and fusion peptides are necessary to induce pore formation but are irrelevant for hemifusion to occur. In contrast, an analogous mutation within the TMD of an H3 subtype (X:31, the same strain used in the present study) did not have an affect on fusion (Armstrong et al., 2000). But low pH causes a much larger fraction of the H3 than the H2

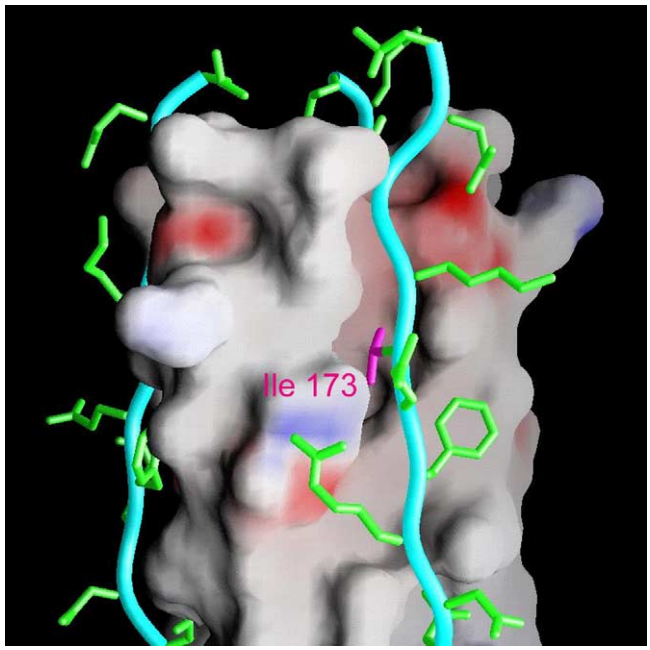

Fig. 9. Interactions of C-terminal residues with the central triple-stranded coiled-coil. The coiled-coil is represented as an opaque molecular surface, colored to denote the surface potential: red for negative, to blue for positive, and white for neutral. The main chain of the C-terminal residues is colored cyan; side chains are colored green, except for 1173, which is colored purple for emphasis. The stretch of coiled-coil between residues 33 and 55 is shown; residues 168–178 of the interacting C-terminii are depicted. A deep hydrophobic pocket, abutted against the N-cap, is created within the grooves of the coiled-coil by T41 and F45 of different monomers. The side chain of I173 from the same monomer as T41 fits into the pocket and hydrogen bonds with Q42 of another monomer. The figure was created with the program GRASP (Nicholls et al., 1991).

subtype of HA to undergo conformational changes (Markovic et al., 2001) and therefore the difference between the strains is possibly due to a greater number of activated copies of the H3 subtype than the H2 subtype. Replacing the TMD with a GPI anchor, or mutating the TMD, or reducing contact between the N-cap and I173 arrests the fusion process at hemifusion, and all should reduce cooperative actions between the TMDs and fusion peptides. The fact that quite different means lead to the same result further supports our central hypothesis that the approach of TMDs and fusion peptides toward each other is the event that generates pore formation.

Materials and methods

Mutagenesis

HA2 mutants were generated by a rapid PCR scheme utilizing Vent polymerase (New England Biolabs, Inc.) which involves amplification of the complete plasmid (Byrappa et al., 1995). The PCR was limited to 12 cycles to minimize the chance of a mistake. For mutants A35E, A35E-A36T, and D37V (in the N-cap region) and 1173E, 1173E-L178Q, V176E, and L178Q (in the C-terminal region), the mutations were made in pSMHAX:31, kindly provided by Dr. Judith White. The *Stu*I/*Xho*I fragment containing each N-cap mutation and the *Xho*I/*Xba*I fragment containing each C-terminal mutation were sequenced using the Big Dye Terminator Cycle Sequencing Ready Reaction Kit (Applied Biosystems, Foster City, CA) before being excised and inserted into pCB6HAX:31, provided by Dr. J. White. Mutants T41K, T41E, 1173Y, and 1173P were directly generated in pCB6HAX:31, using the same PCR method, and the sequence was determined for 500 bp surrounding the mutation.

Expression of wild-type and mutant HA

HEK293T human kidney cells were grown in DMEM (GIBCO-BRL, Gaithersburg, MD) supplemented with 10% Cosmic Calf Serum (Hyclone Laboratories, Logan, UT), 1% penicillin/streptomycin, 1% L-glutamine, and 100 μg/ml of geneticin. The wt HA and mutants were transiently expressed using a standard calcium phosphate transfection method with chloroquine treatment (Luthman and Magnusson, 1983). Unless otherwise indicated, cells were transfected with 6 μg of HA-bearing plasmid per 6-cm dish. Because T41K, T41E, and Δ 173–178 mutants were poorly expressed, here a greater amount of cDNA (24 μg) was used per dish. Cells were used for fusion experiments about 42 h posttransfection. When expression levels had to be further increased, 10 or 25 mM sodium butyrate was added the night before cells were used for experiments (Danieli et al., 1996). Cell surface expression was checked by cell-ELISA (enzyme-linked immunosorbent assay) and FACS, using a primary antibody directed against antigenic Site A (HA1 residues 105–139) (White and Wilson, 1987), provided by Dr. J. White. Point mutants are denoted by standard convention (e.g., I173P). I173-6A signifies a mutant in which all residues from 173 to 178 were mutated to alanine; I173-3A denotes a mutant in which residues 173–175 were mutated to alanine; Δ173–178 signifies a mutant in which the segment 173–178 was deleted.

Cell surface biotinylation, immunoprecipitation, and Western blotting

Biotinylation of cell surface proteins was performed according to published procedures (Qiao et al., 1999). Explicitly, transfected cells on a dish were washed twice with PBS and treated with 1 ml of 1 mg/ml biotin for 45 min at 4°C. Biotin was quenched by 0.05 mM glycine. To cleave HA0, cells were treated with 10 μg/ml TPCK-treated trypsin (Sigma Chemical Co., St. Louis, MO) in PBS for 10 min at room temperature (Qiao et al., 1998). The reaction was stopped by adding an excess of DMEM containing 10% fetal serum for 1 min at RT. Cells were then washed with PBS, lysed in a cell lysis buffer containing 1% NP-40 and a cocktail of protease inhibitors (Delos et al., 2000), and incubated with 1 μg/ml of Site A antibody (White and Wilson, 1987) for 1 h at 4°C with rotation in order to immunoprecipitate HA. Protein A–agarose beads (Pierce Biotechnology, Rockford, IL) were added to and incubated with the lysate for 1 h at 4°C with rotation. The protein A beads were centrifuged at 14,000 rpm for 1 min and sequentially washed with 12.5 mM potassium phosphate, pH 7.4, 0.6 M NaCl, 0.1% SDS, 0.05% NP-40, 0.3 M NaCl, 10 mM Tris, pH 8.3, 12.5 mM potassium phosphate, pH 7.4, 0.3 M NaCl, and finally 20 mM Tris, pH 8.3 (Kemble et al., 1993).

Immune complexes were resuspended in an SDS gel loading buffer (containing 0.14 M β-mercaptoethanol when reducing conditions were required), boiled for 5 min, and separated by 10% SDS–PAGE. Protein was transferred to a nitrocellulose membrane that was then blocked with superblotto (0.5% Tween 20, 10% glycerol, 3% BSA wt/vol, 18% glucose, and 1% dry mild in PBS) and probed with streptavidin–HRP (horseradish peroxidase) as described previously (Qiao et al., 1998).

Monitoring HA conformational changes

Low-pH-induced conformational changes of HA were assayed by cell-ELISA. Transfected cells were treated with trypsin to cleave HA0, incubated in fusion buffer (20 mM succinic acid, 100 mM NaCl, 1.5 mM KCl, 2.5 mM $MgCl_2$, 2.5 mM $CaCl_2$) at different pH values at 37°C for 15 min, washed with PBS, and incubated with rabbit CHA-1 antibody (an antibody directed against HA1 98–106 which is completely inaccessible in the native, neutral-pH form) (White and Wilson, 1987) for 1 h at 4°C. Cells were then washed with PBS, fixed with 2% paraformaldehyde for 15

min at 4°C, and incubated with a secondary antirabbit antibody conjugated with HRP for 1 h at 4°C. About 10^5 of these fixed cells were allowed to attach, for 30 min at 4°C, to wells of a 96-well plate coated with polylysine. The solution was removed and 100 μl of a substrate solution (1 mg of *o*-phenylendiamine, 0.1 M sodium citrate, pH 4.5, and 1.5% H_2O_2) was added and incubated for 30–40 min at RT. (The wells had been blocked by 100 μl of 5% fetal bovine serum in PBS for 15 min at 4°C to avoid nonspecific attachment of substrate.) The ELISA plate was read at 450 nm.

Fusion between HA-expressing cells and RBCs

Fusion experiments between HA-expressing cells and freshly collected human RBCs, colabeled with the membrane probe octadecylrhodamine B chloride (R18) and the aqueous dye carboxyfluorescein (CF) (both from Molecular Probes, Inc. Eugene, OR), were performed essentially as previously described (Melikyan et al., 1997, 2000a). In essence, labeled RBCs were bound to HA-expressing cells, fusion was triggered by acidifying to pH 5.0 for 2 min at 37°C, and dye spread was measured 10–15 min after reneutralization. The number of HA-expressing cells that were stained with either membrane or aqueous dye was normalized by the total number of cells with bound RBCs. In electrical measurements, the formation of fusion pores between HA-expressing cells and RBCs was monitored in the whole-cell patch-clamp configuration as described previously (Melikyan et al., 1999). The internal pipette solution was 155Cs glutamate, 5 mM $MgCl_2$, 5 mM BAPTA, 10 mM HEPES, pH 7.25. RBCs were labeled as in dye transfer experiments to match their conditions. Fusion was triggered by locally ejecting an acidic solution onto the HA cell–RBC pair from another pipette of the same composition as the bathing solution (135 mM *N*-methyl-glucamine aspartate, 5 mM $MgCl_2$, 2 mM HEPES, pH 7.2) except that this pipette solution was buffered to pH 5.0 with 20 mM Cs succinate.

Acknowledgments

We thank Dr. Judith White for providing several essential reagents (pSMHAX:31, pCB6HAX:31, and Site A and CHA-I antibodies), without which this study would not have been possible. We greatly benefited from stimulating conversations with Drs. Michael Caffrey and Theodore Jardetzky regarding the structure of HA. We thank Sofya Brener for steady and careful technical support and Dr. Greg Spear for use of his cell sorter. This work was supported by NIH Training Grant T32-07692 (E.B.D.) and NIH Grants RO1 GM-27367 (F.S.C.), GM-53787 (G.B.M.), and AI47213 (M.E.P.).

References

Armstrong, R.T., Kushnir, A.S., White, J.M., 2000. The transmembrane domain of influenza hemagglutinin exhibits a stringent length requirement to support the hemifusion to fusion transition. J. Cell Biol. 151, 425–438.

Baker, K.A., Dutch, R.E., Lamb, R.A., Jardetzky, T.S., 1999. Structural basis for paramyxovirus-mediated membrane fusion. Mol. Cell 3, 309–319.

Bullough, P.A., Hughson, F.M., Skehel, J.J., Wiley, D.C., 1994. Structure of influenza haemagglutinin at the pH of membrane fusion. Nature 371, 37–43.

Byrappa, S., Gavin, D.K., Gupta, K.C., 1995. A highly efficient procedure for site-specific mutagenesis of full-length plasmids using Vent DNA polymerase. Genome Res. 5, 404–407.

Caffrey, M., Cai, M., Kaufman, J., Stahl, S.J., Wingfield, P.T., Covell, D.G., Gronenborn, A.M., Clore, G.M., 1998. Three-dimensional solution structure of the 44 kDa ectodomain of SIV gp41. EMBO J. 17, 4572–4584.

Chan, D.C., Chutkowski, C.T., Kim, P.S., 1998. Evidence that a prominent cavity in the coiled coil of HIV type 1 gp41 is an attractive drug target. Proc. Natl. Acad. Sci. USA 95, 15613–15617.

Chan, D.C., Fass, D., Berger, J.M., Kim, P.S., 1997. Core structure of gp41 from the HIV envelope glycoprotein. Cell 89, 263–273.

Chen, J., Lee, K.H., Steinhauer, D.A., Stevens, D.J., Skehel, J.J., Wiley, D.C., 1998. Structure of the hemagglutinin precursor cleavage site, a determinant of influenza pathogenicity and the origin of the labile conformation. Cell 95, 409–417.

Chen, J., Skehel, J.J., Wiley, D.C., 1999. N- and C-terminal residues combine in the fusion-pH influenza hemagglutinin HA(2) subunit to form an N cap that terminates the triple-stranded coiled coil. Proc. Natl. Acad. Sci. USA 96, 8967–8972.

Chernomordik, L.V., Frolov, V.A., Leikina, E., Bronk, P., Zimmerberg, J., 1998. The pathway of membrane fusion catalyzed by influenza hemagglutinin: restriction of lipids, hemifusion, and lipidic fusion pore formation. J. Cell Biol. 140, 1369–1382.

Cohen, F.S., Markosyan, R.M., Melikyan, G.B., 2002. The process of membrane fusion: nipples, hemifusion, pores, and pore growth. Curr. Top. Membr. 52, 501–529.

Danieli, T., Pelletier, S.L., Henis, Y.I., White, J.M., 1996. Membrane fusion mediated by the influenza virus hemagglutinin requires the concerted action of at least three hemagglutinin trimers. J. Cell Biol. 133, 559–569.

Delos, S.E., Gilbert, J.M., White, J.M., 2000. The central proline of an internal viral fusion peptide serves two important roles. J. Virol. 74, 1686–1693.

Durrer, P., Galli, C., Hoenke, S., Corti, C., Gluck, R., Vorherr, T., Brunner, J., 1996. H+-induced membrane insertion of influenza virus hemagglutinin involves the HA2 amino-terminal fusion peptide but not the coiled coil region. J. Biol. Chem. 271, 13417–13421.

Eckert, D.M., Kim, P.S., 2001. Mechanisms of viral membrane fusion and its inhibition. Annu. Rev. Biochem 70, 777–810.

Eckert, D.M., Malashkevich, V.N., Hong, L.H., Carr, P.A., Kim, P.S., 1999. Inhibiting HIV-1 entry: discovery of D-peptide inhibitors that target the gp41 coiled-coil pocket. Cell 99, 103–115.

Fass, D., Harrison, S.C., Kim, P.S., 1996. Retrovirus envelope domain at 1.7 angstrom resolution. Nat. Struct. Biol. 3, 465–469.

Ferrer, M., Kapoor, T.M., Strassmaier, T., Weissenhorn, W., Skehel, J.J., Oprian, D., Schreiber, S.L., Wiley, D.C., Harrison, S.C., 1999. Selection of gp41-mediated HIV-1 cell entry inhibitors from biased combinatorial libraries of non-natural binding elements. Nat. Struct. Biol. 6, 953–960.

Frolov, V.A., Cho, M., Reese, T.S., Zimmerberg, J., 2000. Both hemifusion and fusion pores are induced by GPI-linked hemagglutinin. Traffic 1, 622–630.

Gruenke, J.A., Armstrong, R.T., Newcomb, W.W., Brown, J.C., White, J.M., 2002. New insights into the spring-loaded conformational change of influenza virus hemagglutinin. J. Virol. 76, 4456–4466.

Hernandez, L.D., Hoffman, L.R., Wolfsberg, T.G., White, J.M., 1996. Virus-cell and cell-cell fusion. Annu. Rev. Cell Dev. Biol. 12, 627–661.

Kemble, G.W., Danieli, T., White, J.M., 1994. Lipid-anchored influenza hemagglutinin promotes hemifusion, not complete fusion. Cell 76, 383–391.

Kemble, G.W., Henis, Y.I., White, J.M., 1993. GPI- and transmembrane-anchored influenza hemagglutinin differ in structure and receptor binding activity. J. Cell Biol 122, 1253–1265.

Kobe, B., Center, R.J., Kemp, B.E., Poumbourios, P., 1999. Crystal structure of human T cell leukemia virus type 1 gp21 ectodomain crystallized as a maltose-binding protein chimera reveals structural evolution of retroviral transmembrane proteins. Proc. Natl. Acad. Sci. USA 96, 4319–4324.

Luthman, H., Magnusson, G., 1983. High efficiency polyoma DNA transfection of chloroquine treated cells. Nucleic Acids Res. 11, 1295–1308.

Markosyan, R.M., Cohen, F.S., Melikyan, G.B., 2000. The lipid-anchored ectodomain of influenza virus hemagglutinin (GPI-HA) is capable of inducing nonenlarging fusion pores. Mol. Biol. Cell 11, 1143–1152.

Markosyan, R.M., Cohen, F.S., Melikyan, G.B., 2003. HIV-1 envelope proteins complete their folding into six-helix bundles immediately after fusion pore formation. Mol. Biol. Cell 14, 926–938.

Markovic, I., Leikina, E., Zhukovsky, M., Zimmerberg, J., Chernomordik, L.V., 2001. Synchronized activation and refolding of influenza hemagglutinin in multimeric fusion machines. J. Cell Biol. 155, 833–844.

McNew, J.A., Weber, T., Parlati, F., Johnston, R.J., Melia, T.J., Sollner, T.H., Rothman, J.E., 2000. Close is not enough: SNARE-dependent membrane fusion requires an active mechanism that transduces force to membrane anchors. J. Cell Biol. 150, 105–117.

Melikyan, G.B., Brener, S.A., Ok, D.C., Cohen, F.S., 1997. Inner but not outer membrane leaflets control the transition from glycosylphosphatidylinositol-anchored influenza hemagglutinin-induced hemifusion to full fusion. J. Cell Biol. 136, 995–1005.

Melikyan, G.B., Lin, S., Roth, M.G., Cohen, F.S., 1999. Amino acid sequence requirements of the transmembrane and cytoplasmic domains of influenza virus hemagglutinin for viable membrane fusion. Mol. Biol. Cell 10, 1821–1836.

Melikyan, G.B., Markosyan, R.M., Roth, M.G., Cohen, F.S., 2000a. A point mutation in the transmembrane domain of the hemagglutinin of influenza virus stabilizes a hemifusion intermediate that can transit to fusion. Mol. Biol. Cell 11, 3765–3775.

Melikyan, G.B., Markosyan, R.M., Hemmati, H., Delmedicao, M.K., Lambert, D.M., Cohen, F.S., 2000b. Evidence that the transition of HIV-1 gp41 into a six-helix bundle, not the bundle configuration, induces membrane fusion. J. Cell Biol. 151, 413–423.

Melikyan, G.B., White, J.M., Cohen, F.S., 1995. GPI-anchored influenza hemagglutinin induces hemifusion to both red blood cell and planar bilayer membranes. J. Cell Biol. 131, 679–691.

Nicholls, A., Sharp, K.A., Honig, B., 1991. Protein folding and association: insights from the interfacial and thermodynamic properties of hydrocarbons. Proteins 11, 281–296.

Presta, L.G., Rose, G.D., 1988. Helix signals in proteins. Science 240, 1632–1641.

Qiao, H., Armstrong, R.T., Melikyan, G.B., Cohen, F.S., White, J.M., 1999. A specific point mutant at position 1 of the influenza hemagglutinin fusion peptide displays a hemifusion phenotype. Mol. Biol. Cell 10, 2759–2769.

Qiao, H., Pelletier, S.L., Hoffman, L., Hacker, J., Armstrong, R.T., White, J.M., 1998. Specific single or double proline substitutions in the "spring-loaded" coiled-coil region of the influenza hemagglutinin impair or abolish membrane fusion activity. J. Cell Biol. 141, 1335–1347.

Richardson, J.S., Richardson, D.C., 1988. Amino acid preferences for specific locations at the ends of alpha helices. Science 240, 1648–1652.

Russell, C.J., Jardetzky, T.S., Lamb, R.A., 2001. Membrane fusion machines of paramyxoviruses: capture of intermediates of fusion. EMBO J. 20, 4024–4034.

Skehel, J.J., Wiley, D.C., 2000. Receptor binding and membrane fusion in virus entry: the influenza hemagglutinin. Annu. Rev. Biochem. 69, 531–569.

Stegmann, T., Delfino, J.M., Richards, F.M., Helenius, A., 1991. The HA2 subunit of influenza hemagglutinin inserts into the target membrane prior to fusion. J. Biol. Chem. 266, 18404–18410.

Sutton, R.B., Fasshauer, D., Jahn, R., Brunger, A.T., 1998. Crystal structure of a SNARE complex involved in synaptic exocytosis at 2.4 Å resolution. Nature 395, 347–353.

Weissenhorn, W., Calder, L.J., Dessen, A., Lauc, T., Skehel, J.J., Wiley, D.C., 1997. Assembly of a rod-shaped chimera of a trimeric GCN4 zipper and the HIV-1 gp41 ectodomain expressed in Escherichia coli. Proc. Natl. Acad. Sci. USA 94, 6065–6069.

Weissenhorn, W., Calder, L.J., Wharton, S.A., Skehel, J.J., Wiley, D.C., 1998. The central structural feature of the membrane fusion protein subunit from the Ebola virus glycoprotein is a long triple-stranded coiled coil. Proc. Natl. Acad. Sci. USA 95, 6032–6036.

White, J.M., Wilson, I.A., 1987. Anti-peptide antibodies detect steps in a protein conformational change: low-pH activation of the influenza virus hemagglutinin. J. Cell Biol. 105, 2887–2896.

Wilson, I.A., Skehel, J.J., Wiley, D.C., 1981. Structure of the haemagglutinin membrane glycoprotein of influenza virus at 3 Å resolution. Nature 289, 366–373.

Zhao, X., Singh, M., Malashkevich, V.N., Kim, P.S., 2000. Structural characterization of the human respiratory syncytial virus fusion protein core. Proc. Natl. Acad. Sci. USA 97, 14172–14177.